

BRIEF REPORT



Vaccination with a nanoparticle E7 vaccine can prevent tumor recurrence following surgery in a human papillomavirus head and neck cancer model

Sonia Domingos-Pereira^a, Vincent Roh^b, Agnès Hiou-Feige^b, Gabriele Galliverti^c, Christian Simon^b, Genrich V. Tolstonog^{b*}, and Denise Nardelli-Haeffliger^{a*}

^aDepartment of Urology, Lausanne University Hospital and University of Lausanne, Lausanne, Switzerland; ^bDepartment of Otolaryngology–Head and Neck Surgery, Lausanne University Hospital and University of Lausanne, Lausanne, Switzerland; ^cSwiss Institute for Experimental Cancer Research, School of Life Sciences, EPFL, Lausanne, Switzerland

ABSTRACT

High-risk human papillomavirus (HPV) encoding E6/E7-HPV oncogenes are responsible for a subgroup of head and neck squamous-cell carcinoma (HNSCC) and thus therapeutic E7-vaccines may be used to control HPV⁺HNSCC tumors. Herein we investigated the effects of an optimized nanoparticle-conjugated E7 long-peptide vaccine adjuvanted with CpG (NP-E7LP) in an orthotopic immunocompetent mouse model of HPV⁺HNSCC which is based on injection of HPV16 E6/E7-expressing mEERL95-cells into the submental space. In absence of surgery, vaccination performed before or after tumor-cell injection decreased tumor growth or prolonged mice survival only marginally, despite the high numbers of vaccine-induced circulating E7-specific IFN- γ -secreting CD8⁺ T-cells. This contrasts with the high-efficacy of NP-E7LP-vaccination reported in the genital and subcutaneous HPV16-E6/E7-expressing TC-1 models. Our data show that in a direct comparison, NP-E7LP-vaccination fully controlled TC-1, but not mEERL95, tumors subcutaneously growing in the flanks. Immune-cell infiltration was 10-fold higher in TC-1-tumors, than in mEERL95-tumors, suggesting that vaccine-induced CD8⁺ T-cells can only poorly infiltrate mEERL95-tumors. Indeed, immunofluorescence staining of orthotopic mEERL95-tumors showed that CD3⁺ T-cells are preferentially located peritumorally. However, when NP-E7LP-vaccination was performed after mEERL95-cell injection, but before resection of primary tumors, no postsurgical recurrence was observed and 100% of the mice survived until the experimental endpoint (day 70) in the NP-E7LP-vaccinated group. In contrast, we observed a 60% recurrence rate and only 35% survival in PBS-vaccinated mice. This suggests that removal of the primary tumor modified the tumor microenvironment, allowing a therapeutic effect of the vaccine-induced anti-tumor response. E7-vaccination combined with surgery may thus benefit patients with HPV⁺HNSCC.

ARTICLE HISTORY

Received 15 February 2021
Revised 29 March 2021
Accepted 31 March 2021

KEYWORDS

HPV; head and neck cancer; E7 nanoparticle vaccination; recurrence post-surgery

Introduction

About 890,000 new cases of head and neck cancer were reported in 2018 worldwide in association with 450'000 deaths, which are largely attributed to the development of recurrent and/or metastatic disease.^{1,2} A distinct subtype of head and neck squamous cell carcinoma (HNSCC) that expresses Human Papillomavirus (HPV⁺HNSCC) is often diagnosed in younger nonsmoking patients at relatively advanced stages and with nodal involvement, which is however associated with a better survival than HPV negative HNSCC.^{3,4} HPV⁺HNSCC develops from infection of the basal cells of the stratified epithelium by high-risk HPV types.⁵ Because expression of E6 and E7 HPV oncogenes in epithelial cells is required for the maintenance of the cancerous phenotype, they represent attractive target antigens for therapy.⁵ We recently showed that conjugation of an HPV16-E7 long peptide to ultra-small polymeric nanoparticles enhanced the antitumor efficacy of therapeutic vaccination in subcutaneous and genital mouse models of HPV⁺ cancers.⁶ Here, we investigated this therapeutic vaccine in a recently established

immunocompetent orthotopic mouse model of HPV⁺HNSCC, which uses the mEERL95 cell line⁷ that originates from the HPV16 E6/E7-expressing mEERL cell line established from mouse oropharyngeal epithelia.⁸ Injection of mEERL95 cells in the submental space results in the development of primary tumors that recapitulate the patterns of human HPV⁺HNSCC local invasion and metastatic spread.⁷ Surgical resection of primary tumors in this model is associated with the development of local recurrences which mimics the situation in human patients. Because combination with different treatment modalities is clearly necessary for patient benefit,^{9,10} we examined the effect of vaccination alone or in conjunction with surgery of the primary tumors.


Material and methods

Mice treatments

Seven to ten-week-old female C57BL/6 wild-type mice (Charles River and Envigo) were used and all experiments were performed in accordance with Swiss law and with

CONTACT Denise Nardelli-Haeffliger  dnardell@hospv.ch  Dpt Urology, CHUV, Bugnon 48, Lausanne, 1011, Switzerland.

*Contributed equally to this work as senior authors

 Supplemental data for this article can be accessed on the [publisher's website](#).

© 2021 The Author(s). Published with license by Taylor & Francis Group, LLC.

This is an Open Access article distributed under the terms of the Creative Commons Attribution-NonCommercial License (<http://creativecommons.org/licenses/by-nc/4.0/>), which permits unrestricted non-commercial use, distribution, and reproduction in any medium, provided the original work is properly cited.

approval of the Cantonal Veterinary Office of Canton de Vaud, Switzerland. The mEERL95 cell line was derived from a tumor explant of the original mEERL cell line⁸ (obtained from Prof. John H. Lee, Sanford Research, Sioux Falls, South Dakota, USA) implanted in a C57BL/6 female mouse.⁷ The TC-1 cell line (C57BL/6 primary lung epithelial cells transduced with retroviral vectors expressing HPV16 E6/E7 and activated c-Ha-ras)¹¹ was kindly provided by Prof. T.-C. Wu (Johns Hopkins Medical Institutions, Baltimore, USA). Subcutaneous vaccination was performed with NP-E7LP (15 µg of synthetic E7₄₃₋₇₇ peptide, chemically synthesized by the Protein and Peptide Chemistry Facility of the Institute of Biochemistry, UNIL, Switzerland, conjugated in nanoparticle (NP) as detailed in⁶ and 40 µg of CpG: CpG-B 1826 oligonucleotide 5'-TCCATGAGCTTCCTGACGTT-3' as phosphorothioated DNA bases, purchased from Microsynth). Briefly, NPs were synthesized, functionalized, and characterized and then incubated for 12 hours in endotoxin-free water and guanidine hydrochloride with E7₄₃₋₇₇ dissolved in DMSO. E7 NP were purified by size-exclusion chromatography using CL-6B matrix (Sigma Merck KGaA), eluted, and stored in PBS at room temperature, 40 µg of CpG were added before vaccination (NP-E7LP vaccine). Control vaccinations were also performed with PBS or CpG (40 µg) alone.

Tumor implantation and surgery

For orthotopic tumors, 100'000 mEERL95 cells were injected into the cervical subcutaneous tissue (the submental space) as previously described.^{7,12,13} For flank tumors, 100'000 mEERL95 and 100'000 TC-1 cells were subcutaneously implanted on each flank of the mice. Tumor growth was monitored with a Vernier caliper, and tumor volume was calculated as $V = (L \times W^2)/2$. Procedure for surgery at the neck region were previously detailed.^{7,14} Briefly, with the help of a stereomicroscope, tumors were dissected and wounds were closed with a suture. At the time of surgery, tumor invasion of the bone and muscle were recorded.

Tissues preparation

Mice were sacrificed by CO₂ inhalation to collect the tumor tissues. Single-cell suspensions were obtained by mincing in DL-dithiothreitol (Sigma Merck KGaA) and digesting with 1 mg/mL collagenase/dispase (Roche, Basel, Switzerland) and 0.1 mg/ml DNase I (Sigma Merck KGaA) with 20% Fetal Calf Serum (Gibco, MA, USA). Whole blood was collected in tubes containing heparin-Na 25000 I.E. (Braun, Sempach, Switzerland) from tail vein. Red blood cells were lysed using ammonium-chloride-potassium. PBMC were prepared from tail-blood.¹⁵ The recovered cells were used for immunostaining and/or for IFN-γ ELISPOT assay.

Immunostaining and flow cytometry analysis

The monoclonal anti-mouse antibodies used were Anti-CD45-FITC (30-F115), Anti-CD3-PerCP/Cy5.5 (17A2), Anti-CD11b-AF700 or eF450 (M1/70) and Anti-CD4-eF450 (GK1.5), (eBioscience, Thermo Fisher Scientific, MA, USA),

Anti-CD8-APC-Cy7 (53-6.7), Anti-Ly6C-AF700 (HK1.4) and Anti-Ly6G-Pe-Cy7 (1A8) (Biolegend, CA, USA). PE-conjugated E7₄₉₋₅₇-H-2 D^b-restricted tetramers (tetE7) were from Ludwig Institute for Cancer Research tetramer production facility, Lausanne, Switzerland. Dead cells were excluded by a live/dead fixable aqua dead cell stain kit (Invitrogen Thermo Fisher Scientific, MA, USA). Cell acquisition and analysis were performed using Gallios Flow Cytometer (Beckman Coulter, Nyon, Switzerland) and FlowJo software (Tree Star, Ashland, OR), respectively.

Immunofluorescence staining was performed on OCT frozen sections using hamster mCD3e antibody (BD 550277) and rabbit E-cadherin antibody (Cell Signaling 3195). Briefly, sections were fixed 10 minutes at RT with 4% PFA, permeabilized 10 minutes at RT with 0.1% Triton X-100 then blocked 30 minutes in PBS 0.5% BSA containing 1% goat and 1% donkey serum before incubation for 2 hours at RT with a 1/100 dilution of mCD3e antibody and a 1/400 dilution of E-cadherin antibody in 0.5% BSA/PBS. After incubating 1 hour at RT with donkey anti-rabbit-647 (Life Technologies A-31573) and goat anti-hamster-568 (Life Technologies A-21112) antibodies diluted 1/500 in 0.5% BSA/PBS, sections were mounted in ProLong Gold antifade reagent with DAPI (Life technologies P-36931) and digitalized on an Axio Scan.Z1 (Zeiss). Fiji software was used to quantify immunofluorescence signals using custom scripts.

IFN-γ ELISPOT assay

IFN-γ ELISPOT assay were performed as described in detail in.¹⁵ Briefly, 100'000 PBMC/well were loaded with 1 µg/ml of E7₄₉₋₅₇ peptide (synthesized by the Protein and Peptide Chemistry Facility, UNIL, Lausanne, Switzerland) or medium alone (control wells). After 16 to 24 h. E7-specific responses were defined for each individual mouse as the number of IFN-γ spots/10⁵ cells in the E7-stimulated wells minus the number of IFN-γ spots/10⁵ cells in the control wells.

Statistics

Statistical analyses were performed using Prism 7.00 for Windows (GraphPad software). Single comparisons were performed using Student t-test or Chi-square contingency test. Multiple comparisons were performed using one-way ANOVA and Tukey's post-test or log-rank test as indicated in the figure legends.

Results and discussion

NP-E7LP vaccination decreased orthotopic mEERL95 tumor growth and prolonged mice survival only slightly

We first examined the effect of the optimized HPV16-E7 long-peptide vaccine conjugated to ultra-small polymeric nanoparticles and adjuvanted with CpG (NP-E7LP⁶) in the orthotopic mEERL95 model in the absence of surgery. Groups of mice were vaccinated at days 5 and 15 after tumor cell injection with NP-E7LP (n = 16), CpG alone (n = 9) or PBS (n = 10) (Figure 1a). Both NP-E7LP and the CpG adjuvant alone

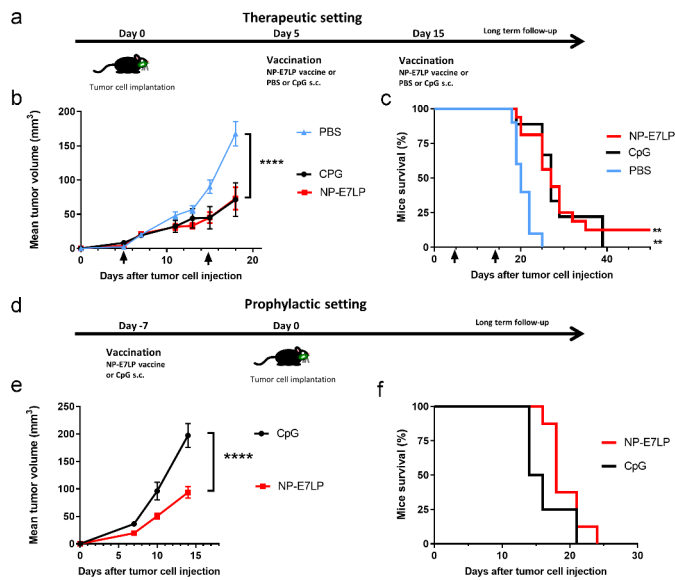


Figure 1. Growth of orthotopic mEERL95 tumors and mice survival upon therapeutic or prophylactic vaccination. a-c: In a therapeutic setting, mice with orthotopic mEERL95 tumors were vaccinated at day 5 and 15 (black arrow in b/c) with PBS (n = 10), CpG alone (n = 9) or NP-E7LP (n = 16). d-f: In a prophylactic setting, mice were vaccinated 1 week before cell injection with CpG alone (n = 8) or NP-E7LP (n = 8). Mean \pm SEM tumor growth (b/e) and mice survival (c/f) are shown. Significant differences (area under the curve, a/c) are shown following Student t-test or (mice survival, c/f) after an adjusted log-rank test: **** = $p < .0001$; ** = $p < .01$.

significantly decreased tumor growth rate (Figure 1b) and prolonged mice survival, as compared to PBS-injected mice (Figure 1c). As expected, NP-E7LP induced significantly higher numbers of E7-specific IFN- γ secreting CD8 T-cells in peripheral blood mononuclear cells (PBMC) after the first or second

immunization than in mice that had received CpG alone or PBS (supplementary Figure 1s). These results confirm that the CpG adjuvant alone has immunotherapeutic properties that can confer some tumor protection,¹⁶ but also question the importance of the vaccine-induced E7-specific CD8⁺ T-cells in this setting. When vaccination with NP-E7LP was performed 1 week before orthotopic tumor cell injection (Figure 1d), there was a significant decrease in tumor growth, as compared to CpG alone (Figure 1e). This confirmed that the E7-expressing mEERL95 tumors are sensitive to the vaccine-induced E7-specific CD8⁺ T-cells, in agreement with previous findings with the parental cell line mEER^{17,18} though with no benefit on mice survival (figure 1f). These results contrast with the previously reported efficacy of subcutaneous (s.c.) vaccination with NP-E7LP to control tumors in the E7-expressing TC-1 s.c. and genital models.^{6,10} This may be due to vaccine-specific CD8⁺ T-cells not efficiently homing to the tumor site (in this case the floor of the mouth) and/or the presence of a higher immunosuppressive tumor microenvironment in the orthotopic mEERL95 tumors. To test these possibilities, we directly compared groups of mice which were s.c. implanted on each flank with TC-1 or mEERL95 cells and vaccinated s.c. 1 week later with NP-E7LP or CpG alone (Figure 2a). In this setting, TC-1 tumors, in the NP-E7LP vaccination group, fully regressed at day 30 (Figure 2b), while mEERL95 tumor growth was only slightly decreased, as compared to CpG alone (Figure 2c); this despite the presence of a high number of circulating E7-specific IFN- γ secreting CD8⁺ T-cells (Figure 2d). This suggests that it is not the localization of the mEERL95 tumors that interfered with vaccine efficacy. Interestingly, flow-cytometry analysis of flank mEERL95 and TC-1 tumors (see gating strategy in Supplementary Figure 2), showed a significantly lower

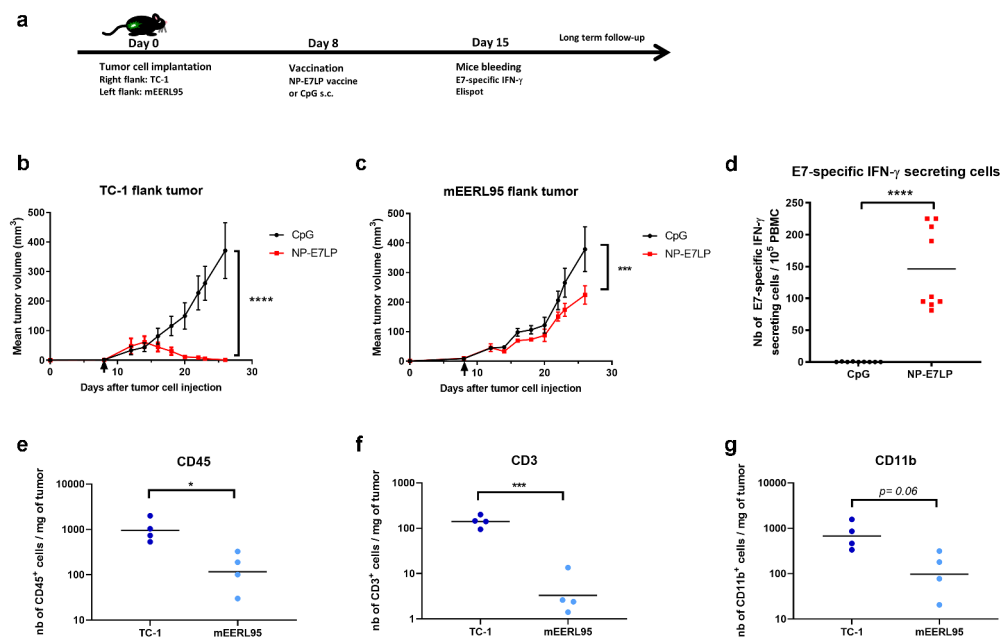


Figure 2. Growth and immune responses of flank TC-1 and mEERL95 tumors upon therapeutic vaccination. a: TC-1 and mEERL95 tumors were subcutaneously established on each flank of the mice (n = 18) and vaccination was performed 7 days later (black arrow in b/c) with the NP-E7LP (n = 9) or CpG alone (n = 9), mice bleeding was performed at day 15. Growth curves (mean \pm SEM tumor volumes) of TC-1 (b) and mEERL95 (c) tumors are shown separately. d: Number IFN- γ E7-specific CD8 T-cells were measured in PMBC, 7 days after vaccination. e-g: Numbers of tumor-infiltrating immune cells/mg of tumor were determined in mice sacrificed at day 19 (n = 4) by flow cytometry for CD45 (e) CD3 (f) and CD11b (g). Significant differences (area under the curve for b/c) are shown following Student t-test, **** = $p < .0001$. *** = $p < .001$, ** = $p < .01$ and * = $p < .05$.

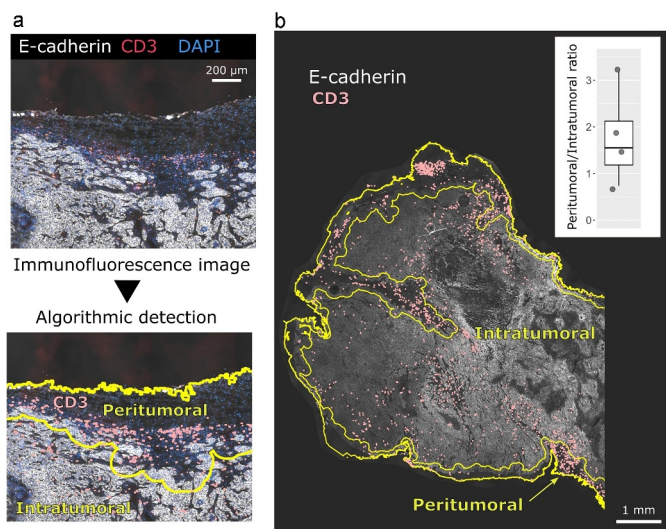


Figure 3. CD3 cells are mainly located peritumorally in the orthotopic mEERL95 tumors. **a:** Example of the algorithmic detection of CD3 and E-cadherin immunostaining signal on frozen sections from orthotopic mEERL95 tumors. The epithelial-specific E-cadherin and nuclear DAPI signals are used to accurately define the peritumoral and intratumoral areas of the sample. **b:** Overview of a whole tumor section showing that CD3 T-cells are preferentially found in the peritumoral area. (**inset**): Quantification of the ratio between CD3 T-cells detected in the peritumoral area versus CD3 T-cells detected in the intratumoral area in PBS treated mice ($n = 4$).

infiltration of CD45⁺ immune cells (Figure 2e), particularly affecting the CD3⁺ T-cells (50-fold decrease, $p < .001$, figure 2f) and to a lesser extent the CD11b⁺ myeloid cells (fivefold decrease, $p = .06$, Figure 2g), in mEERL95 tumors, as compared to TC-1 tumors. Both CD4⁺ and CD8⁺ T-cells similarly

decreased in mEERL95 tumors, with Tetramer E7⁺ CD8⁺ T-cells only detected in the TC-1 tumors (supplementary Figure 3s A, B, C), while among the myeloid cells, only the Ly6C⁺ CD11b⁺ cells (a phenotype of monocyte-derived suppressor cells) were significantly decreased in the mEERL95 tumors (supplementary Figure 3s D/E). These data suggest that lack of efficacy of circulating vaccine-induced E7-specific CD8⁺ T-cells may be associated with a poor immune cell infiltration in the mEERL95 tumors, irrespective of their localization. Indeed, quantitative digital analysis of immunostained lateral cross-sections obtained from orthotopic mEERL95 tumors (Figure 3a) revealed a spatially confined infiltration of the E-cadherin-positive tumor areas by CD3⁺ T-cells, which were preferentially enriched around the tumors and in the stromal invaginations (Figure 3b) resulting in a mean peritumoral/intratumoral infiltration ratio of 1.5 (Figure 3b, inset). Of note, the mEERL95 tumor model is characterized by the presence of a desmoplastic stroma rich in cancer-associated fibroblasts (CAFs),⁷ which were shown to interfere with T-cell infiltration and be a barrier to vaccination.¹⁹ Whether CAFs are responsible for the low immune cell infiltration in the mEERL95 model deserves further investigations.

NP-E7LP vaccination performed before surgical resection of primary tumors prevents local recurrence

Because NP-E7LP vaccination alone was poorly efficient in our model, we then exploited the possibility to surgically remove the primary orthotopic mEERL95 tumors to test a combination treatment. Groups of mice injected with mEERL95 cells were

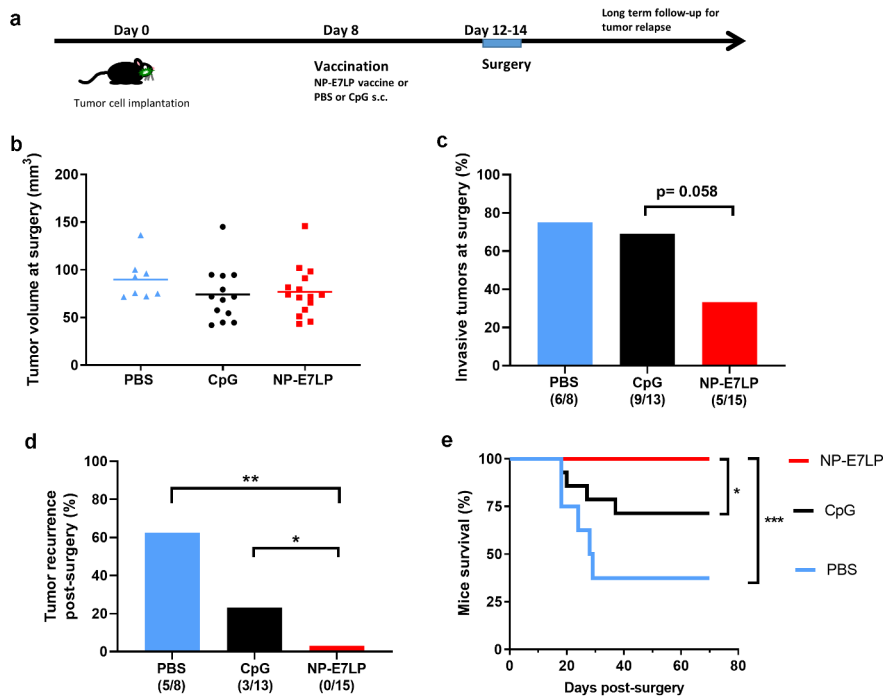


Figure 4. Growth and local recurrence of orthotopic mEERL95 tumors upon combined NP-E7LP vaccination and surgery. Groups of female mice bearing orthotopic mEERL95 tumors were vaccinated with NP-E7LP ($n = 15$), CpG alone ($n = 13$) or PBS ($n = 8$) before resection of the primary tumors as outlined in **a**. Tumor volumes (**b**) and percentage of muscle and/or bone invasive tumors (**c**) at surgery are shown. After surgery, percentage of mice with postsurgical recurrence (**d**) and mice survival (**e**) are shown. Significant differences following one-way ANOVA + Tukey's posttest (**b**), contingency Chi-square test (**c-d**) or log-rank test (**d**) are shown: * = $p < .05$, ** = $p < .01$, *** = $p < .001$.

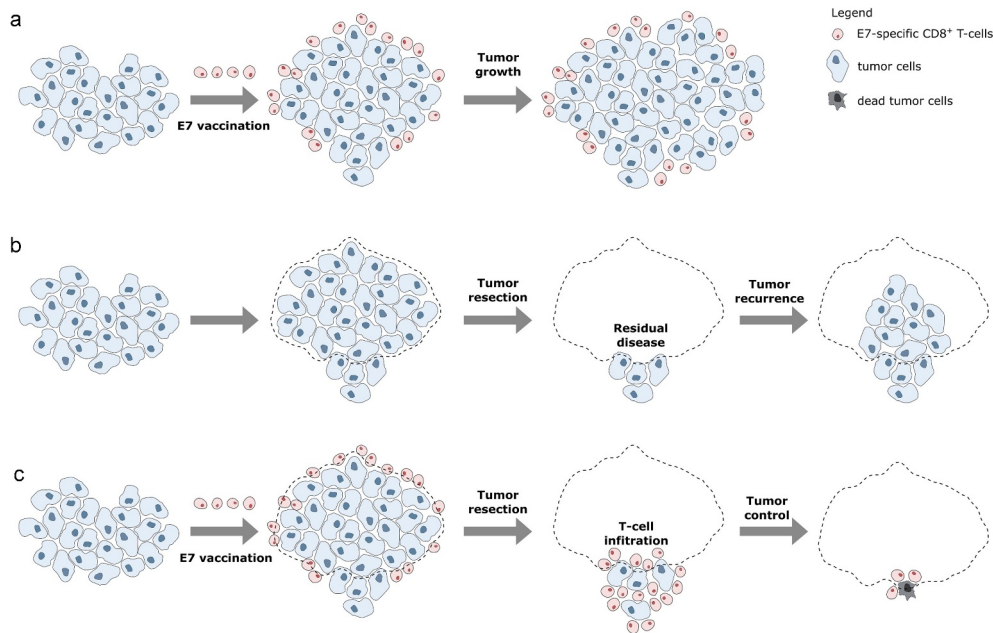


Figure 5. Working principles of E7 vaccination prior to tumor resection. **a:** When E7 vaccination is performed after tumor cell injection, circulating E7-specific CD8⁺ T-cells are induced. However, these cells cannot infiltrate the tumor which continues to grow. **b:** After resection of primary tumors, residual tumor cells can regrow resulting in tumor recurrence. **c:** Primary tumor resection performed after E7 vaccination allows circulating E7-specific CD8⁺ T-cell to infiltrate the residual tumor cells and efficiently control the tumor, thus impeding tumor recurrence.

vaccinated 8 days later with NP-E7LP ($n = 15$), CpG alone ($n = 13$) or PBS ($n = 8$) and, 12–14 days after implantation, primary tumors were surgically removed and mice were followed for tumor recurrence (Figure 4a). Tumor volumes at the time of surgery were similar (Figure 4b), but visual inspection showed that muscle and/or bone invasion was less frequent after NP-E7LP vaccination (33%, $p = .058$, as compared to CpG) than in controls (ca. 70% for either PBS or CpG, Figure 4c). This suggests that the modest effect on tumor growth by NP-E7LP vaccination or CpG alone which is only evident at later time points in absence of surgery (see Figure 1b), may only be partly associated with a lesser propensity of the tumor to invade. Notably, no postsurgical tumor recurrence was observed in NP-E7LP-vaccinated mice (0/15), as opposed to a significant recurrence rate (3/13 and 5/8) in the CpG and PBS controls, respectively (Figure 4d). This resulted in 100% mice survival at the endpoint (day 70) for the NP-E7LP-vaccinated mice which was significantly better than for CpG or PBS controls (70% and 37% mice survival, respectively, Figure 4e). This suggests that the vaccine-induced E7-specific IFN- γ secreting cells effectively controlled local recurrence after resection of primary tumor (Figure 5). We may speculate that removing most of the tumor, including CAFs, has exposed residual tumor cells to the preexisting vaccine-induced T-cells allowing their effect before the burden of dysfunctional immune responses often associated with surgery.²⁰

Conclusion

Although the implementation of prophylactic HPV-vaccines may decrease the occurrence of HPV⁺HNSCC in the future,²¹ their incidence is still rising in several countries.^{22,23} In addition, despite HPV⁺HNSCC generally better responds to treatment than cancers unrelated to HPV, a subgroup still shows recurrence with a poor

survival prognosis,²⁴ which deserves optimized treatment strategies. Using the orthotopic mEERL95 tumor model that mimic such a situation, our data show that an E7-vaccine can beneficially be included in the therapy of aggressive HPV⁺HNSCC, when administered before the resection of the primary tumor.

Acknowledgments

We are thankful to Prof. Doug Hanahan for his strong support and the interesting discussions throughout this project and to the institutional Animal, Mouse Pathology, Cellular Imaging and FACS facilities for their excellent assistance.

The study was funded by the Swiss National Science Foundation (#CRII3 160742 to CS and DNH and #310030_152875 to GVT), by Swiss Cancer Research (KFS 4103022017 to DNH and KFS-4726-02-2019 to GVT) and by the Faculty of Biology and Medicine (FBM) of the University of Lausanne (to CS).

Disclosure of interest

The authors report no conflict of interest.

Funding

The study was funded by the Swiss National Science Foundation (#CRII3 160742 to CS and DNH and #310030_152875 to GVT), by Swiss Cancer Research (KFS 4103022017 to DNH and KFS-4726-02-2019 to GVT) and by the Faculty of Biology and Medicine (FBM) of the University of Lausanne (to CS).

References

1. Bray F, Ferlay J, Soerjomataram I, Siegel RL, Torre LA, Jemal A. Global cancer statistics 2018: GLOBOCAN estimates of incidence and mortality worldwide for 36 cancers in 185 countries. *CA Cancer J Clin.* 2018;68(6):394–424. doi:10.3322/caac.21492.

2. Johnson DE, Burtneß B, Leemans CR, Lui VWY, Bauman JE, Grandis JR. Head and neck squamous cell carcinoma. *Nat Rev Dis Primers*. 2020;6:92.
3. Marur S, D'Souza G, Westra WH, Forastiere AA. HPV-associated head and neck cancer: a virus-related cancer epidemic. *Lancet Oncol*. 2010;11(8):781–789. doi:10.1016/S1470-2045(10)70017-6.
4. Taberna M, Mena M, Pavon MA, Alemany L, Gillison ML, Mesia R. Human papillomavirus-related oropharyngeal cancer. *Ann Oncol*. 2017;28(10):2386–2398. doi:10.1093/annonc/mdx304.
5. Zur Hausen H. Papillomaviruses and cancer: from basic studies to clinical application. *Nat Rev Cancer*. 2002;5(5):342–350. doi:10.1038/nrc798.
6. Galliverti G, Tichet M, Domingos-Pereira S, Hauert S, Nardelli-Haeßler D, Swartz MA, et al. Nanoparticle conjugation of Human Papillomavirus 16 E7-long peptides enhances therapeutic vaccine efficacy against solid tumors in mice. *Cancer Immunol Res*. 2018;6(11):1301–1313. doi:10.1158/2326-6066.CIR-18-0166.
7. Mermoud M, Hiou-Feige A, Bovay E, Roh V, Sponarova J, Bongiovanni M, et al. Mouse model of postsurgical primary tumor recurrence and regional lymph node metastasis progression in HPV-related head and neck cancer. *Int J Cancer*. 2018;142(12):2518–2528. doi:10.1002/ijc.31240.
8. Hoover AC, Spanos WC, Harris GF, Anderson ME, Klingelutz AJ, Lee JH. The role of human papillomavirus 16 E6 in anchorage-independent and invasive growth of mouse tonsil epithelium. *Archives of Otolaryngology–head & Neck Surgery*. 2007;133(5):495–502. doi:10.1001/archotol.133.5.495.
9. Van Der Burg SH, Arens R, Ossendorp F, Van Hall T, Melief CJ. Vaccines for established cancer: overcoming the challenges posed by immune evasion. *Nat Rev Cancer*. 2016;16(4):219–233. doi:10.1038/nrc.2016.16.
10. Domingos-Pereira S, Galliverti G, Hanahan D, Nardelli-Haeßler D. Carboplatin/paclitaxel, E7-vaccination and intravaginal CpG as tri-therapy towards efficient regression of genital HPV16 tumors. *J Immunother Cancer*. 2019;7(1):122. doi:10.1186/s40425-019-0593-1.
11. Lin KY, Guarnieri FG, Staveleyocarrroll KF, Levitsky HL, August JT, Pardoll DM, et al. Treatment of established tumors with a novel vaccine that enhances major histocompatibility class II presentation of tumor antigen. *Cancer Res*. 1996;56(1):21–26.
12. Simon C, Hicks MJ, Nemechek AJ, Mehta R, O'Malley BW Jr., Goepfert H, et al. PD 098059, an inhibitor of ERK1 activation, attenuates the in vivo invasiveness of head and neck squamous cell carcinoma. *Br J Cancer*. 1999;80(9):1412–1419. doi:10.1038/sj.bjc.6690537.
13. Simon C, Nemechek AJ, Boyd D, O'Malley BW Jr., Goepfert H, Flaitz CM, et al. An orthotopic floor-of-mouth cancer model allows quantification of tumor invasion. *The Laryngoscope*. 1998;108(11 Pt 1):1686–1691. doi:10.1097/00005537-199811000-00018.
14. Behren A, Kamenisch Y, Muehlen S, Flechtenmacher C, Haberkorn U, Hilber H, et al. Development of an oral cancer recurrence mouse model after surgical resection. *Int J Oncol*. 2010;36(4):849–855. doi:10.3892/ijo_00000562.
15. Revaz V, Debonneville A, Bobst M, Nardelli-Haeßler D. Monitoring of vaccine-specific gamma interferon induction in genital mucosa of mice by real-time reverse-transcription-PCR. *Clin Vacc Immunol*. 2008;5(5):757–764. doi:10.1128/ CVI.00392-07.
16. Temizoz B, Kuroda E, Ishii KJ. Vaccine adjuvants as potential cancer immunotherapeutics. *Int Immunol*. 2016;28(7):329–338. doi:10.1093/intimm/dxw015.
17. Lee DW, Anderson ME, Wu S, Lee JH. Development of an adenoviral vaccine against E6 and E7 oncoproteins to prevent growth of human papillomavirus-positive cancer. *Archives of Otolaryngology–head & Neck Surgery*. 2008;134(12):1316–1323. doi:10.1001/archoto.2008.507.
18. Dharmaraj N, Piotrowski SL, Huang C, Newton JM, Golfman LS, Hanoteau A, et al. Anti-tumor immunity induced by ectopic expression of viral antigens is transient and limited by immune escape. *Oncoimmunology*. 2019;8(4):e1568809. doi:10.1080/2162402X.2019.1568809.
19. Wang C, Dickie J, Sutavani RV, Pointer C, Thomas GJ, Savelyeva N. Targeting head and neck cancer by vaccination. *Front Immunol*. 2018;9:830. doi:10.3389/fimmu.2018.00830.
20. Market M, Baxter KE, Angka L, Kennedy MA, Auer RC. The potential for cancer immunotherapy in targeting surgery-induced natural killer cell dysfunction. *Cancers*. 2018;11(1):1. doi:10.3390/cancers11010002.
21. Chaturvedi AK, Graubard BI, Broutian T, Pickard RKL, Tong ZY, Xiao W, et al. Effect of Prophylactic Human Papillomavirus (HPV) Vaccination on Oral HPV infections among young adults in the United States. *J Clin Oncol: Off J Am Soc Clin Oncol*. 2018;36(3):262–267. doi:10.1200/JCO.2017.75.0141.
22. Chaturvedi AK, Engels EA, Pfeiffer RM, Hernandez BY, Xiao W, Kim E, et al. Human papillomavirus and rising oropharyngeal cancer incidence in the United States. *J Clin Oncol: Off J Am Soc Clin Oncol*. 2011;29(32):4294–4301. doi:10.1200/JCO.2011.36.4596.
23. Shewale JB, Gillison ML. Dynamic factors affecting HPV-attributable fraction for head and neck cancers. *Curr Opin Virol*. 2019;39:33–40. doi:10.1016/j.coviro.2019.07.008.
24. Harbison RA, Kubik M, Konnick EQ, Zhang Q, Lee SG, Park H, et al. The mutational landscape of recurrent versus nonrecurrent human papillomavirus-related oropharyngeal cancer. *JCI Insight*. 2018;3(14):14. doi:10.1172/jci.insight.99327.